



OPEN

DATA DESCRIPTOR

Psilocybin's acute and persistent brain effects: a precision imaging drug trial

Subha Subramanian¹✉, Travis Rick Renau², Demetrius Perry², Ravi Chacko³, Timothy O. Laumann², Karin Flavin², Christine Horan⁴, Julie Schweiger², Nicholas Metcalf⁵, Eric J. Lenze², Abraham Z. Snyder^{5,6} , Nico U. F. Dosenbach^{5,6,7,8,9}, Ginger Nicol^{2,11} & Joshua S. Siegel^{10,11}✉

Psilocybin (PSIL) is a psychedelic drug and a promising experimental therapeutic for many psychiatric conditions. Precision functional mapping (PFM) combines densely repeated resting state fMRI sampling and individual-specific network mapping to improve signal-to-noise ratio (SNR) and effect size in brain imaging research. We present a randomized cross-over study in which PFM was used to characterize acute and persistent effects of psilocybin or methylphenidate (MTP) on brain networks. Seven healthy volunteers (mean age 34.1 years, SD = 9.8; n = 3 females, n = 6 Caucasians) underwent (1) extensive baseline imaging, (2) imaging beginning 60–90 minutes after drug exposure, and (3) longitudinal imaging for up to two weeks after drug exposure. Four individuals also participated in an open-label PSIL replication protocol over 6 months later. This dataset includes resting state (using advanced high-resolution multi-echo fMRI), task fMRI, structural, and diffusion basis spectral imaging as well as assessments of subjective experience. We are releasing this unique dataset as a resource for neuroscientists to study the acute and persistent effects of PSIL and MTP on brain networks.

Background & Summary

Psilocybin (PSIL) is a serotonin receptor 2A (5-HT_{2A}) agonist that has shown positive, rapid benefits in clinical trials for numerous psychiatric indications, including depression^{1–4}, end-of-life anxiety^{5,6}, obsessive compulsive disorder⁷, eating disorders^{8,9}, and alcohol use disorder^{10–12}. These trials have found immediate (hours to days) and persistent (weeks to months) benefit from a single dose, making PSIL a promising treatment with broad applications in psychiatry.

The neurobiological mechanisms of PSIL's immediate and persistent effects remain an active and important area of investigation. Persistent effects include increases in positive mood and the personality domain of openness^{13,14}. The discussion on therapeutic mechanisms of psychedelic drugs has focused on the acute subjective psychological experience, including the profound mystical experience frequently reported by individuals undergoing psychedelic therapy. However, to understand how these drugs produce a persistent clinical response (i.e., post-acute drug effects), it is necessary to understand circuit adaptations underlying a drug's psychological effects.

Functional magnetic resonance imaging (fMRI) has been used to explore the effects of psychedelic compounds on human brain circuits¹⁵. Recent studies using MRI to probe acute effects of psychedelics have reported

¹Department of Psychiatry, Beth Israel Deaconess Medical Center and Harvard Medical School, Boston, MA, 02215, USA. ²Department of Psychiatry, Washington University School of Medicine in St. Louis, St. Louis, MO, USA. ³Department of Emergency Medicine, Advocate Christ Medical Center, Oak Lawn, IL, USA. ⁴Miami VA Medical Center, Miami, FL, USA. ⁵Department of Neurology, Washington University School of Medicine, St Louis, MO, USA. ⁶Mallinckrodt Institute of Radiology, Washington University School of Medicine, St Louis, MO, USA. ⁷Department of Biomedical Engineering, Washington University in St. Louis, St Louis, MO, USA. ⁸Department of Pediatrics, Washington University School of Medicine, St Louis, MO, USA. ⁹Department of Psychological & Brain Sciences, Washington University in St. Louis, St. Louis, MO, USA. ¹⁰Department of Psychiatry, NYU Langone Center for Psychedelic Medicine, NYU Grossman School of Medicine, New York, NY, USA. ¹¹These authors contributed equally: Ginger Nicol, Joshua S. Siegel. ✉e-mail: ssubram5@bidmc.harvard.edu; Joshua.Siegel@nyulangone.org

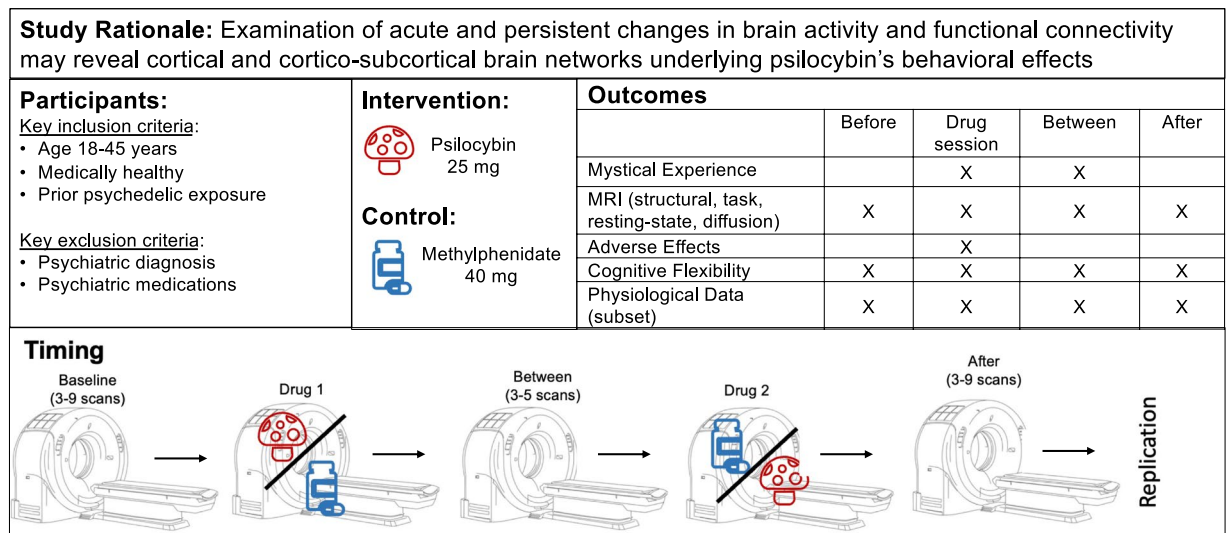


Fig. 1 Graphical abstract: PICOT (Participants, Intervention, Control, Outcomes, Timing). This study recruited healthy adults with previous psychedelic exposure. Participants were enrolled in a cross-over study design using a precision functional mapping (PFM) approach. Key inclusion and exclusion criteria are listed, see methods section for complete list of criteria. Outcomes included subjective experiences, cognitive flexibility, and extensive MRI (including structural, task-based, resting state, and diffusion). MRI sequences were performed before the first drug, during the first and second drug, between the first and second drug, and after the second drug. A subset of participants also wore pulse oximeter and respiratory belt during MRIs for physiological assessments. Four out of seven participants completed the replication protocol.

decreases in functional connectivity in the default mode network^{15,16} and an overall decrease in fMRI signal power across the cortex^{17,18}. Psychedelic brain imaging continues to face challenges and limitations. Individual variability, head motion, autonomic arousal, and changes to vascular and/or neurovascular coupling^{19,20} have been potential confounds in prior fMRI studies accessing acute psychedelic effects.

To overcome these aforementioned limitations, we applied a series of neuroimaging advancements that we have termed “precision imaging drug trial” (PIDT). PIDT builds on the principals of precision functional mapping – using dense repeated sampling and individualized network mapping and analysis – to account for inter-individual variability and overcome many limitations of conventional resting state fMRI²¹. Precision functional mapping has revealed new details of cortical and subcortical brain network organization obscured by conventional group-average techniques^{21–24} and large within-participant changes in network organization following an intervention²⁵.

We recruited healthy adults to participate in a cross-over PIDT trial comparing brain effects of PSIL (25 mg dose) or active placebo (methylphenidate, MTP, 40 mg dose) (Fig. 1). Seven individuals underwent dense repeated sampling with resting state and task-based fMRI before, after, and during drug exposure. To assess variability of PSIL's effects within and across individuals, four participants received a second open-label dose of PSIL after six months (“replication protocol”).

Our PIDT approach implemented Framewise Integrated Real-time MRI Monitoring (FIRMM), multi-echo EPI imaging, Nordic thermal de-noising, monitoring and regression of physiological signals (pulse-ox, respiratory belt) to provide state-of-the-art data quality and spatial resolution of longitudinal connectomics measurements.

Here, we present a dataset suited to explore a range of questions about the individual differences and shared effects of PSIL on brain networks. This dataset substantially expands the existing body of available psychedelics fMRI data. As McCullough *et al.* point out in their review, over 50% of the published literature on psychedelics effects on rsfMRI are based on two data sets¹⁵. This may be due to the barriers involved in researching psychedelic compounds. To aid other scientists interested in creating similar datasets, we summarize study challenges and potential solutions to such research in Supplementary Table 1.

Using this dataset, we recently reported that: (1) Acutely, PSIL produced context-dependent desynchronization of brain activity, and individual differences were strongly linked to the subjective psychedelic experience. (2) Persistent decreases in hippocampus-default mode network connections were observed up to three weeks after, suggesting a neuroanatomical and mechanistic correlate of PSIL's long-term effects²⁶.

Methods

Study design and rationale. We designed a randomized controlled cross-over study (Fig. 1), using a PIDT design to evaluate individual-level brain connectivity pre-, post- and during PSIL or MTP exposure. Healthy adults were selected as the study population to reduce potential confounds from psychiatric diagnoses and/or medications. To reduce negative effects of drug exposure on participant experience, anticipatory anxiety, and imaging quality, participants were required to have had at least one previous lifetime psychedelic exposure and

no psychedelic exposure in the six months before study participation. Usona Institute, a United States non-profit medical research organization with FDA authorization to produce medical-grade PSIL²⁷, provided PSIL 25 mg pills.

Participants underwent two separate imaging sessions during active drug exposure: one with PSIL (25 mg) and one with MTP (40 mg). Drug sessions were spaced one to two weeks apart. MTP was selected as the active control condition to match the cardiovascular effects and physiological arousal (i.e., controlling for dopaminergic effects on blood pressure and heart rate) associated with PSIL¹³. Six months after completing the initial study, participants were invited to participate in a replication protocol including a baseline fMRI and another dose of PSIL (25 mg) with brain imaging.

Two clinical research staff who completed the Usona Institute facilitator training program facilitated the drug sessions. The role of the study facilitators was to build a rapport with the participant throughout the study, prepare them for their drug dosing days, and monitor participant safety during dosing day visits. The facilitation pair consisted of a trained clinician (J.S.S. and S.S.) and a trainee (D.P. and C.H.).

At least three non-drug imaging sessions were completed before, between and after drug sessions (e.g., at least nine non-drug imaging sessions total). Dosing day imaging sessions started 60 minutes after drug administration and lasted ~120 minutes, spanning the period of peak blood concentration^{28–30}. The number of non-drug sessions was dependent on availability of the participant, scanner, and scanner support staff. Scans occurred at the same time of day for each participant.

Inclusion/exclusion criteria. Healthy adults between the ages of 18 and 45 years with previous psychedelic exposure (>6 months prior to enrollment) were recruited via campus-wide advertisement and colleague referral. Participants were enrolled from March 2021 to March 2023. Exclusion criteria included: contraindications to MRI scanning (e.g., bone hardware, implantable devices, IUD); contraindications to PSIL exposure (e.g., cardiovascular disease, hypertension, renal disease, neurological condition, or pregnancy); diagnosis of psychiatric condition (including substance use disorders); current use of any psychotropic medication (e.g., TCAs, SSRIs, SNRIs, MAOIs, antipsychotics, lithium, valproate, tramadol); previous adverse reactions to psychedelics; immediate family history of any psychotic disorder (e.g., schizophrenia spectrum or psychotic mood disorders).

Study measures. After providing informed consent, participants underwent screening tests, including an electrocardiogram, urine drug screen, basic metabolic panel, complete blood count and a urine pregnancy test. A study physician acquired a medical history, performed a physical exam, and reviewed labs to ensure that participants did not have exclusionary health conditions. Once medically cleared, participants were scheduled for imaging sessions and drug dosing days to ensure appropriate timing of pre-, post-, and dosing day scans (see ‘Imaging visits’ and ‘Medication visits’ below). Supplementary Table 2 illustrates the study’s schedule of activities.

Scales and questionnaires. Assessments were conducted before, during, and after treatment sessions. Subjective data and objective measures of the medication experiences were collected, as well as a personality survey and safety parameters. Assessments obtained are described below:

International personality item pool-five-factor model (Mini-IPIP). The Mini-IPIP is a 20-question staff-administered survey to determine the Big Five factors of an individual’s personality: extraversion, agreeableness, conscientiousness, neuroticism, and openness to experience³¹. The Mini-IPIP was administered at the following time points: baseline, post-drug one, and post-drug two.

Mystical experience questionnaire (MEQ). The MEQ30 is a 30-item self-reported questionnaire that measures mystical experiences. It measures four factors: a) mystical (freedom from boundaries of one’s personal self and a feeling of unity to what is greater than one’s self), b) positive mood (sense of awesomeness or awe), c) transcendence of time and space (being outside of real of time), d) ineffability (sense that experience cannot be described well in words)^{14,32}. The MEQ30 was administered at the following time points: baseline, post-drug one, post-drug two. We administered the MEQ30 on the same day of drug administration.

Challenging effects questionnaire. This self-report questionnaire evaluates challenging experience with psychedelics (panic or fear, grief, isolation, feeling as though one is dying, feeling insane, physiological distress, and paranoia)³³. It was administered as part of the pre-screening phone assessment to determine eligibility, and was repeated 24 hours post-drug one and post-drug two.

Emotional breakthrough inventory. This is a 6-item survey that was used to assess if the psychedelic experience produced an emotional breakthrough³⁴.

Imaging visits. For each participant, all imaging visits were scheduled at the same approximate time of day (e.g., morning, afternoon, evening) to minimize time-of-day effects. The goal was to have visits occurring on days 1–2, 3–4, 5–7, and ~14 after each drug. For replication protocol visits, the goal was to have at least one MRI visit before and one visit after PSIL dose.

MRI Acquisition. MRI scanning was conducted on a Siemens Prisma MRI scanner (Siemens, Erlangen, Germany). Imaging session timelines are illustrated in Fig. 1. Imaging sessions included a combination of structural MRI (T1- and T2-weighted images), two or more resting state fMRI scans (513 frames, 15 minutes each), and two sessions of task fMRI scans (233 frames, 6 minutes and 50 seconds each). Structural scans were obtained at 0.9 mm isotropic resolution. Resting state and task scans used an echoplanar imaging sequence with multi-echo (five TEs: 14.20 ms, 38.93 ms, 63.66 ms, 88.39 ms, 113.12 ms), TR 1761 ms, flip angle = 68 degrees,

and in-plane acceleration (IPAT/grappa) = 2^{35,36}. This sequence acquired 72 axial slices (144 mm coverage). For resting state and task fMRI, three frames at the end were utilized to estimate electronic noise^{37,38}.

During all imaging sessions, FIRMM was used to provide feedback on head motion during scanning^{39,40} and eye tracking was used to ensure that participants remained awake. Participants were provided with feedback about head motion between scans.

Resting state fMRI. During resting state fMRI scans, participants were instructed to visually fixate on a white crosshair presented on a grey background. We aimed to acquire a minimum of two 15-minute resting state fMRI scans per visit. Given that optimal data cleaning has been shown to remove up to 25% of the data¹⁸, 30 minutes of multi-echo resting state fMRI was necessary to measure cortico-subcortical networks²³.

Task based fMRI. During some MRI visits, participants completed two event-related fMRI task scans. This was a suprathreshold auditory-visual matching task in which participants were presented with a naturalistic visual image (duration 500 ms) and coincident spoken English phrase. They were asked to respond with a button press to indicate if the image and phrase were ‘congruent’ (for example, an image of a beach, and the spoken word “beach”) or ‘incongruent’. Both accuracy and response time of button presses were recorded. Each trial was followed by a jittered inter-stimulus interval optimized for event-related designs. Task fMRI scans employed the same sequence used in resting fMRI, included 48 trials (24 congruent, 24 incongruent), and lasted 410 seconds each.

Diffusion MRI and diffusion basis spectrum imaging (DBSI). Given that increasing evidence suggests that psychedelics work as potent anti-inflammatory agents⁴¹, coupled with the key role inflammation plays in psychiatric illnesses^{42,43}, we acquired diffusion MRI using sequences optimized for diffusion basis spectrum imaging (DBSI). This included acquisitions with b-values of 1500 and 3000, each with 102 directions (TR=3500ms, TE = 83 ms) – identical to sequences being used in ABCD⁴⁴. DBSI models inflammation-associated cellularity (DBSI-restriction fraction, RF) and vasogenic edema (DBSI-hindered fraction, HF) while accounting for partial volume effects resulting from cerebrospinal fluid contamination and crossing fibers^{45,46}. Diffusion scans on PSIL were omitted if there were time constraints or to mitigate a participant’s comfort level.

Physiological assessments. A subset of participants wore a Siemens built-in respiratory belt and a pulse oximeter during all MRI sessions (Table 1). Prior to MRI scanning, a belt was placed around the individual’s thorax, with the sensor just below the ribcage. A pulse oximeter was placed on the non-dominant index finger. All data from respiratory belt and pulse oximeter were preprocessed using PhysIO⁴⁷ to extract pulse- and respiration-based metrics, fMRI-aligned time courses, as well as physiological regressors for nuisance regression of fMRI data.

Preparation and integration sessions. In addition to undergoing MRI sessions, preparation and integration sessions were held in a dedicated research treatment room where the study drug was also administered. Preparatory sessions were held one or two days before drug administration. Integration sessions were held one day after drug administration. The purpose of preparatory sessions was to build a therapeutic alliance between facilitators and participants. The participant’s personal history, developmental stage, current life situation, and intentions for and expectations of drug sessions were reviewed. Integration sessions involved discussing experiences that emerged throughout the dosing session and the day after drug exposure. Preparation and integration sessions occurred per Usona clinical study guidelines.

Drug dosing visits. *Drug administration.* Participants received either 25 mg of PSIL or 40 mg of MTP. Both facilitators and subjects were blinded. Medications were taken with water and lemon ginger tea. Mindfulness occurred for 10 minutes, and then participants were invited to lie on the sofa with eye shades as well as headphones. A curated psychedelic music sequence played through the headphones to reduce external stimulation. One hour after drug administration, participants were transported to the MRI suite wearing headphones and eye shades. Following the MRI, participants were transported back to the dedicated testing room and encouraged to direct their attention internally until subjective drug effects were completely resolved. Study facilitators then completed a modified post-session integration checklist with participants. Dosing sessions for both drugs were 7–8 hours in length.

Patient safety and monitoring. As both PSIL and MTP impact cardiac and vascular functioning, heart rate and blood pressure were measured at regular intervals during dosing days (e.g., 30, 60, 90, 120, 180, 240, 300, 360, 420, and 480 minutes after drug ingestion). At these intervals, we queried participants about adverse effects, including time of onset, time of resolution, event description, and whether intervention was required. Rescue medications (risperidone for agitation, lorazepam for anxiety, and niacin for chest pain) were available as needed. The Columbia Suicide Severity Rating Scale (C-SSRS) was used to assess for suicidal ideation and behavior during drug exposure⁴⁸. Participants had access to a physician who was physically present throughout dosing day.

Treatment guess. After each medication dosing, participants were asked to guess whether they received PSIL or MTP.

Regulatory approvals & registrations. This study was approved by the Washington University Human Research Protection Office (WU HRPO), the Federal Drug Administration (IND: 02002165) and the Missouri

Participant Number	1	2	3	4	5	6	7
Participant Demographics							
Biological sex	Male	Male	Female	Female	Male	Female	Male
Age (years)	44	38	36	37	19	22	43
Last degree completed	BA/BS	BA/BS	BA/BS	MA/MS/PhD	HS/GED	BA/BS	MA/MS/PhD
Last psychedelic exposure (months)	24	24	12	24	24	12	60
Completed replication	Yes	No	No	Yes	Yes	Yes	No
Number of MRI Scans^a							
15-minute rsfMRI, without PSIL	34 [11]	36	30 [6]	27 [7]	31 [7]	21	26
15-minute rest fMRI, on PSIL	2 [4]	2	1 [3]	1 [2]	4 [3]	2	6
15-minute rest fMRI, on MTP	2	2	2	3	4	3	3
7-minute task fMRI, no drug	12 [2]	12	10 [0]	10 [2]	2 [4]	6	12
7-minute task fMRI, PSIL	2 [2]	2	2 [0]	2 [2]	0 [2]	1	2
7-minute task fMRI, MTP	2	2	2	2	0	2	2
DBSI, no drug	10	7	8	12	11	3	5
DBSI, PSIL	2	0	2	1	2	0	1
DBSI, MTP	0	0	1	1	1	1	0
Physiological Data							
Blood Pressure, (no drug, PSIL, MTP)	Yes	Yes	Yes	Yes	Yes	Yes	Yes
Electrocardiogram (no drug)	Yes	Yes	Yes	Yes	Yes	Yes	Yes
Screening Labs	Yes	Yes	Yes	Yes	Yes	Yes	Yes
Respiration & heart rate, in scanner	Partial ^b	No	Partial ^b	Yes	Yes	Yes	Yes
Behavioral Data							
MEQ30	Yes	Yes	Yes	Yes	Yes	Yes	Yes
MINI-IPIP	Yes	Yes	Yes	Yes	Yes	Yes	Yes
Substance use questionnaire?	Yes	Yes	Yes	Yes	Yes	Yes	Yes

Table 1. Demographic, neuropsychological and behavioral data. ^aNumber scans acquired during initial enrollment. Number of scans acquired during replication are enclosed with square brackets “[]”. ^bDenotes individuals who have some, but not complete, physiological data.

Drug Enforcement Agency (DEA) under a federal DEA schedule 1 research license and registered with clinicaltrials.gov (NCT04501653). Synthetic PSIL was supplied by Usona Institute via Almac Clinical Services.

Data management. De-identified assessment scores, raw data from structural MRI and fMRI scans was uploaded into the Central Neuroimaging Data Archive (CNDA).

rsfMRI processing and surface projection. Preprocessing of fMRI data included: (1) removal of thermal noise using NORDIC (a local PCA approach in which temporal components of an fMRI signal that are indistinguishable from Gaussian noise are eliminated)^{37,38,49}; (2) sync interpolation to correct asynchronous slice acquisition; (3) affine spatial registration of all volumes within a run; (4) exclusion of odd/even slice intensity differences from interleaved acquisition (debanding); (5) compute affine spatial registration across fMRI runs; (6) compute an run volume mean (of all low-noise volumes); (7) field distortion correction on the basis of a spin echo field maps using FSL top-up⁵⁰; and (8) gain field correction based on run volume mean using FSL fast⁵¹ (computed on the run volume mean).

Resampling in MNI152 2 mm³ atlas space was accomplished for all echoes in one step combining (i) motion correction; (ii) distortion correction; (iii) gain field correction; (iv) linear registration of average volumes across visits; and (v) non-linear MNI152 atlas registration via the FSL FNIRT^{52–55}. The multi-echo data in MNI152 space then were combined using the weighted summation approach (as described in Posse *et al.* equations 6 and 7⁵⁶).

After cross-modal registration, the data underwent several pre-processing steps. These included: FreeSurfer segmentation for tissue-based regression, elimination of signals with false variance, temporal filtering to include 0.009–0.08 Hz bands, and frame censoring⁵⁷. False signals included: six parameters obtained by rigid body correction of head motion, extra-axial noise, white matter, and ventricles. Frame censoring was performed on all resting state fMRI data at FD > 0.30 mm⁵⁵.

After preprocessing, BOLD data was analyzed using each participant’s cortical surface and nuclei. Voxels with high coefficients of variation were excluded from volume to surface mapping⁵⁴. Resting data was then sampled into a set of about 385 brain regions using a previously validated parcellation of cortical (324) and sub-cortical (61) brain areas^{21,23}. These regions can be used for functional connectivity analysis.

Data analysis. The primary goal of our study was to test significant differences between baseline and PSIL scans using a within-participant design, followed by testing if differences replicate across participants. For the

present data resource, we conducted descriptive analytics on the participant population using behavioral assessments and physiological data. We also assessed imaging quality via assessing whole brain network similarity matrices and brain modularity.

Physiological measurements were recorded at 400 Hz with clocked timestamps and extracted using PhysIO Toolbox⁴⁷ as raw plethysmography signals. All signals were visually inspected and entire sessions were rejected if significant clipping occurred or if signals were noisy, without regular oscillations expected in pulse or respiratory plethysmography. We calculated instantaneous pulse rate (PR) and respiratory rate (RR) by labeling the peaks and troughs of the wave using Matlab's findpeaks function, and we then calculated pulse rate or respiratory rate between each peak. This custom rate calculation agreed with PhysIO toolbox for respiratory rate but offered higher temporal resolution with respect to pulse rate. Physiological regressors for fMRI analyses were created using the automated PhysIO Toolbox. A mixed linear effects model was used to determine the relative effects of MTP and PSIL on the session means of physiological parameters.

For similarity matrix correlation calculations were performed at the parcel level. The effects of condition (baseline, PSIL, between, MTP, after), and participant were directly examined by calculating the similarity between each functional network matrix (i.e., Pearson correlation between the linearized upper triangles of the parcellated FC matrix between a pair of 15 minute fMRI scans), creating a second-order “similarity” matrix⁵⁸.

Spectral power in the infra-slow band (0.009 to 0.06 Hz) was evaluated in each parcel as the cosine Fourier transform of the BOLD signal autocovariance function computed in a manner that allows for motion censoring⁵⁹. Spectral power was averaged over cortical parcels to generate a single value for each session.

Modularity (Newman's Q) was calculated using the equation⁶⁰:

$$Q = \sum_{\mu \in M} \left[e_{\mu\mu} - \left(\sum_{\nu \in M} e_{\mu\nu} \right)^2 \right]$$

where the network (including nodes and binary undirected links) is fully subdivided into a set of nonoverlapping modules M , and $e_{\mu\nu}$ is the proportion of all links that connect nodes in module μ with nodes in module ν . Matlab code to calculate modularity and other graph measures (below) was taken from the Brain Connectivity Toolbox⁶¹, publicly available at sites [google.com/site/bctnet/](https://www.google.com/site/bctnet/).

A linear mixed effects model with random effects for participant and MRI session was used to test the effect of drug condition (PSIL, MTP, baseline, and post-PSIL) on modularity and BOLD infraslow power.

Let y_{ij} be the rs-fMRI metric (e.g. FC change score at a given vertex) for the j -th observation (15-minute fMRI scan) within the i -th participant. The linear mixed-effects model can be written as:

$$y_{ij} = \beta_0 + \beta_{\text{drug}} \cdot \text{drug}_{ij} + \beta_{\text{FD}} \cdot \text{FD}_{ij} + \beta_{\text{task}} \cdot \text{task}_{ij} + \beta_{\text{task*drug}} \cdot \text{task}_{ij} \cdot \text{drug}_{ij} + u_{0i} + v_{0j} + \varepsilon_{ij}$$

- β_0 is the intercept term.
- β_{drug} , β_{FD} , β_{task} and $\beta_{\text{task*drug}}$ are the coefficients for the fixed effects predictors.
- drug_{ij} , FD_{ij} , and task_{ij} are the values of the fixed effects predictors for the j -th observation within the i -th group.
- u_{0i} represents the random intercept for the i -th participant, accounting for individual-specific variability.
- v_{0j} represents the random intercept for the j -th observation within the i -th participant, capturing scan-specific variability.
- ε_{ij} is the error term representing unobserved random variation.

Data Record

Repository information. All imaging data (raw, minimally preprocessed, and fully processed) for participants (P1-P7) and replication sessions (P1R, R3R, P4R, P5R) are available on OpenNeuro (OpenNeuro Dataset ds006072, <https://openneuro.org/datasets/ds006072>)⁶². All participants consented to have their data shared on a publicly available archive. Images are in Nifti format, defaced, and in BIDS structure⁶³. Each participant has a folder containing subfolders with each scanning session. Within each session folder, “anat,” “dwi,” “fmap,” and “func” folders are present. Scanning dates, MRI sequences, and scan notes and complications are presented in “PPFM_session_notes.xlsx” file in OpenNeuro. Scanning notes include: time frames in which participants may have fallen asleep, high degrees of head motion, FIRR complications, scanner malfunction, and respiratory belt malfunction. Behavioral assessments such as mystical experiences and personality factors are provided in the folder “Behavioral Assessments”. We briefly summarize demographic, behavioral, movement, and physiological data below.

Participant demographics and characteristics. Seven adults consented and completed the study (mean age of 34.1 years, SD = 9.8). Three individuals were female, and six were Caucasian. Additional baseline characteristics of the study population are included in Table 1. See Supplementary Fig. 1 for participant disposition.

Subjective experiences and adverse events. Overall, self-reports of mystical experiences on PSIL vs. MTP (active placebo) were significantly higher ($p < 0.05$) across all four mystical factors. Average mystical, positive mood, transcendence, and ineffability domain scores (out of 5 points) were: 3.4 vs. 0.61, 3.8 vs. 1.2, 3.8 vs. 0.33, and 3.7 vs. 0.86 for PSIL vs. placebo, respectively (Fig. 2).

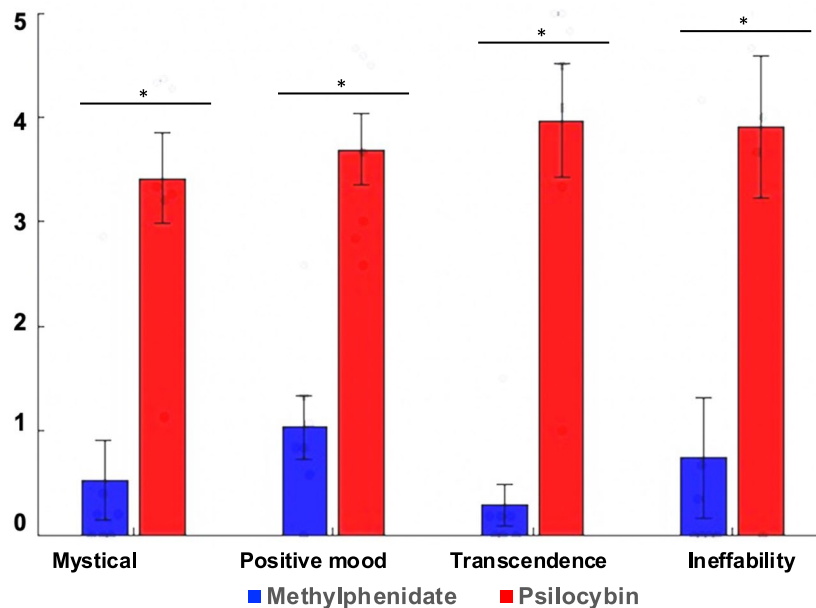


Fig. 2 Mystical Experiences Questionnaire (MEQ30) results. Data presented are mean and standard deviations of measurement in all seven participants. Participants were asked to look back on their drug experience on the same day of receiving PSIL or MTP and rate the degree to which they experienced criteria across five factors (transcendence, positive mood, ineffability, mystical) from a scale of 0 to 5. A score of 0 indicates did not experience at all, and a score of 5 is given to extremely experienced (more than any other time in their life). Asterisks: * $p < 0.05$, two-tailed t-test.

One participant (P3) reported a higher MEQ30 score on MTP vs. PSIL. Specifically, this participant reported higher ineffability (4.2 vs. 0), transcendence (1.5 vs 1), and mystical experience (2.8 vs. 1.1) on MTP vs. PSIL. Positive mood was scored the same on both MTP and PSIL. When this participant came back for the replication protocol (i.e., received a second dose of PSIL), she obtained higher mystical experience scores: 4.1 on ineffability, score 5.0; transcendence, 2.1; mystical experience, 4.4, and positive mood, 4.1. P3 was the only participant who incorrectly guessed when they received PSIL and MTP on participant blinding questionnaires (e.g., stated “positive I received [active or placebo] drug”). Individuals stated that the multiple baseline scans prior to drug exposure improved the comfortability of being on a psychedelic in the MRI scanner.

Four to six hours after PSIL ingestion, side effects reported included: 14% headache [$n = 1$], 28% nausea [$n = 2$], 28% anxiety [$n = 2$]. No serious adverse events occurred while participants were on PSIL or MTP and undergoing MRI. No participant required rescue medications.

MRI data quantity and head motion. Because psychedelics increase head movement, training participants beforehand to remain still and comfortable in the scanner was critical for the collection of behaviorally relevant brain-wide signals. Thus, participants underwent 4–9 non-drug MRI visits prior to their first drug imaging session and FIRMM was used to provide participants feedback about head motion at each session. Consequently, compared with prior psychedelics imaging datasets, participants were able to provide a greater quality (Fig. 3a,b) and quantity (Fig. 3c) of data while still achieving a mystical experience on PSIL (Fig. 2).

Combining the protocol + replication visits, we obtained an average of 39.4 (SD = 12.2) “off drug” 15-minute resting state scans from 7 participants (Table 1). We obtained an average of 4.7 (SD 2.0) 15-minute resting state scans on PSIL per participant and 2.7 (SD = 0.8) 15-minute resting state scans on MTP.

In this PIDT study, 86% ($n = 6$ out of 7) had at least one usable 15-minute resting scan on PSIL (i.e., frame-wise head motion was ≤ 0.2 mm). Only participant P2 did not. By comparison to prior PSIL dataset (Fig. 3), in Carhart-Harris *et al.* 2012 study of PSIL⁶⁴, 46% ($n = 7$ out of 15) had any usable resting state data (any scan with average framewise head motion less than or equal to 0.2 mm). In Carhart-Harris *et al.* 2016 study of LSD, 75% ($n = 15$ out of 20) had one resting state scan meeting framewise head motion requirements¹⁸.

Physiological data. Pulse and respiratory rates obtained during fMRI scans were analyzed within and across participants and conditions (Fig. 4). Within participant, baseline sessions (before drug 1) were used as the control condition to assess for both effect of drug and after-drug on pulse and respiratory rate. Changes were observed in drug conditions (MTP, PSIL) but no consistent changes were observed in off-drug conditions (between, after). Thus, for group-level analyses, non-drug sessions were combined and a mixed linear effects model was used to assess effects of MTP and PSIL on the physiological parameters. The average baseline pulse rate was 72 beats per minute (bpm, 95% CI, 68–77) and the respiratory rate was 11 respirations per minute (rpm, 95% CI, 9–13). A mixed linear effects model was used to determine the relative effects of MTP and PSIL on the session means of physiological parameters. On average, MTP was associated with a 16.7 bpm increase in pulse rate (95%

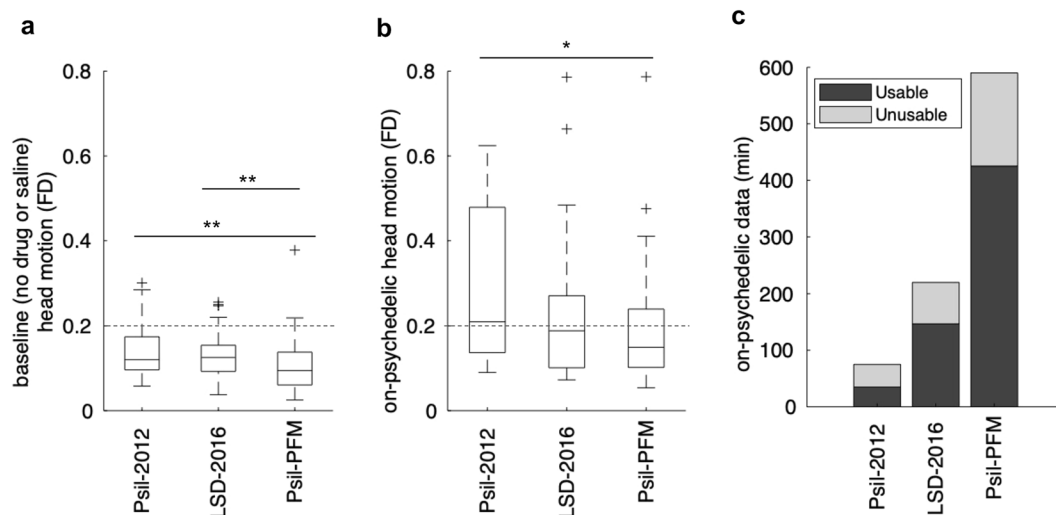


Fig. 3 Comparison of head motion to prior psychedelic fMRI datasets. Average head motion (framewise displacement, FD in millimeters) for each scan off (a) and on (b) psychedelic drug was compared between our dataset and prior psychedelic fMRI studies^{18,64}. In a/b, the dotted line at 0.2 mm represents a stringent cutoff for exclusion of a session. Sessions with average FD of 0.2 mm or lower are considered usable. Lower and upper quartiles of box-plots were calculated as follows: $Q1 - 1.5 \times IQR$, $Q3 + 1.5 \times IQR$, respectively. Asterisks indicate significant ($* p < 0.05$, $** p < 0.005$, unpaired t-test, two tailed) difference in head motion compared to two other highly cited datasets^{18,64}. (c) The totality of resting state data (usable and unusable) on psychedelic in minutes.

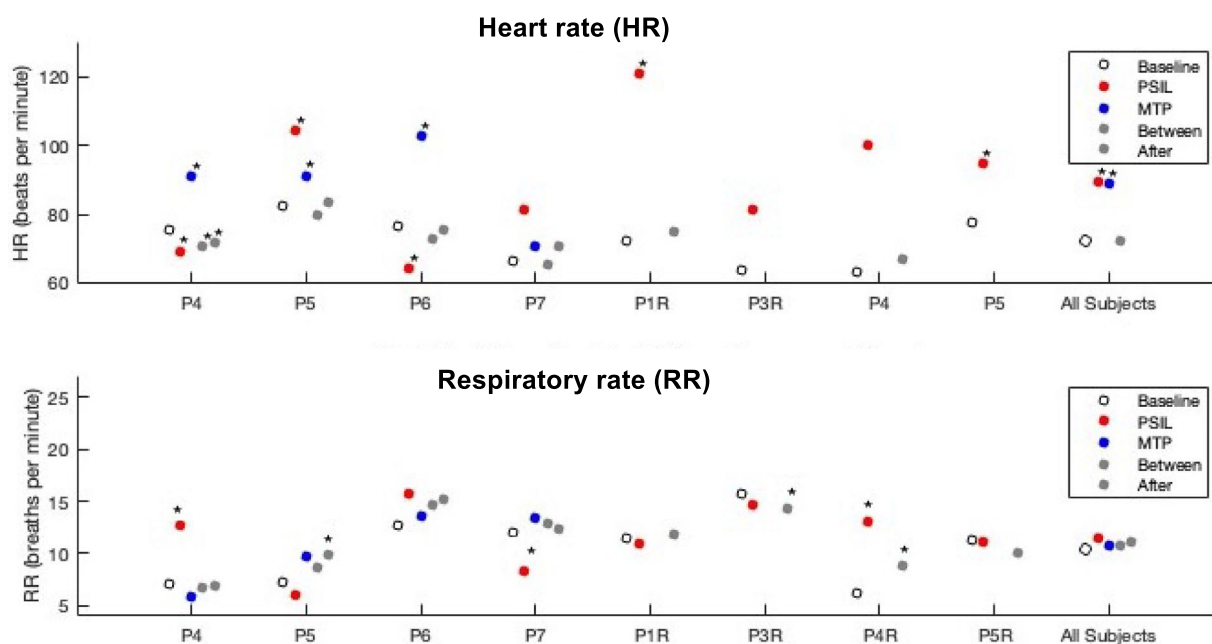


Fig. 4 Physiological data within and across participants based on drug condition. Heart rate (HR, beats per minute) and respiratory rate (RR, breaths per minute) for each participant based on drug condition for each participant (including replication visits). Empty circles represent physiological measures averaged across all baseline sessions for a participant, red dots represent physiological measures during PSIL, blue dots are physiological measure on MTP, and gray dots represent averages for between and after sessions. To determine if a given condition differed significantly from baseline, a linear mixed effects model was used. $HR = 199$ observations, MTP-baseline Estimate (95% CI) = 16.7 bpm (11.0, 20.3), $t_{(196)} = 6.6$, $P_{\text{uncorr}} = 3.12 \times 10^{-10}$; PSIL-baseline Estimate (95% CI) = 21.1 bpm (16.6, 25.6), $t_{(196)} = 9.2$, $P_{\text{uncorr}} = 4.04 \times 10^{-17}$. No significant difference in HR was observed between MTP and PSIL ($p_{\text{uncorr}} = 0.399$). $*p < 0.001$, uncorrected.

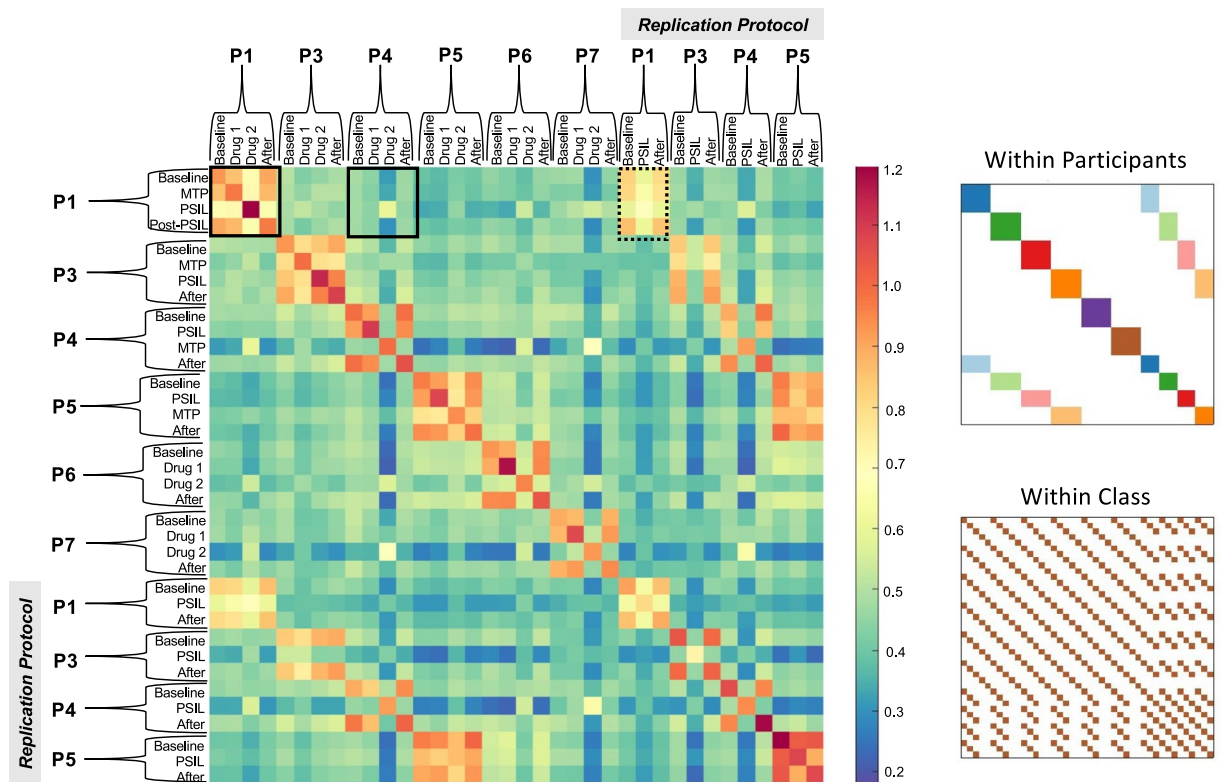


Fig. 5 Whole brain network similarity matrix and intra-subject data reliability. Each row and column represent brain networks (average FC matrix) from one participant in one study condition (baseline, Drug 1, between, Drug 2, after) and each edge represents similarity of functional networks between a pair of conditions. Networks from the replication protocol are shown at the end of the matrix. The diagonal represents the similarity between all scans within the same classification (e.g., all baseline scans for P1). Note: for MTP and PSIL sequences, fMRI comparisons are among resting state scans acquired during that same ‘on drug’ MRI sequence. To the right, a visualization of data structure demonstrates two sources of similarity – ‘within participant’ and ‘within class’ (e.g. brain networks from two participants’ PSIL condition). For example, Participant 1’s whole brain functional networks without and on drug sessions are similar when compared to themselves vs. Participant 4 (see solid black squares in chart). When Participant 1 came back for replication, their whole brain functional networks on PSIL were highly correlated to their replication session on PSIL six months later (see dotted box in chart). Participant 2 was excluded, given a large degree of unusable data (framework head displacement > 0.2 mm).

CI:11.0–20.3, $p_{LME} = 3.12 \times 10^{-10}$). PSIL was associated with a 21.1 bpm increase in pulse rate (95% CI 16.6–25.6, $p_{LME} = 4.04 \times 10^{-17}$). No significant difference in HR was observed between MTP and PSIL ($p = 0.399$).

Technical Validation

Similarity matrix and modularity. To explore macro trends in the data, we visualized whole-brain connectome similarity within and across participants (Fig. 5)^{21,58}. The 5×5 red boxes observed along the diagonal demonstrate the overall similarity within-participant across sessions (as indicated by ‘Within Participant’. And the 3×5 red rectangles on the top right and lower left corners represent within participant similarity when participants returned for replication protocol 6–12 months later. The PSIL condition stands out as substantially less like other conditions (including MTP) in every subject. Interestingly, there is PSIL-PSIL similarity within and across participants (suggested a shared effect of PSIL, as described in Siegel *et al.*²⁶).

Network modularity, a measurement of brain-network segregation, was recently shown to significantly decrease in individuals with treatment-resistant depression following treatment with PSIL⁶⁵. In our dataset, network modularity decreased from baseline during PSIL ($P = 1.8754 \times 10^{-9}$) but did not remain significantly changed in the weeks following PSIL (Fig. 6; $P = 0.68$). MTP also had no significant effect on modularity ($P = 0.85$).

Intraparticipant reliability. To assess variability in effects of PSIL within-participant across doses, four participants underwent a second PSIL dose 6–12 months after their initial dose (including at least one MRI visit before and after dosing). Baseline, during PSIL, and post-PSIL rsfMRI, diffusion, structural, and task-based MRI were conducted. When individuals came back for the replication protocol, the second PSIL dose produced similar whole brain network changes (similarity to replication $r = 0.78$, similarity across participants $r = 0.45$, $P < 0.001$).

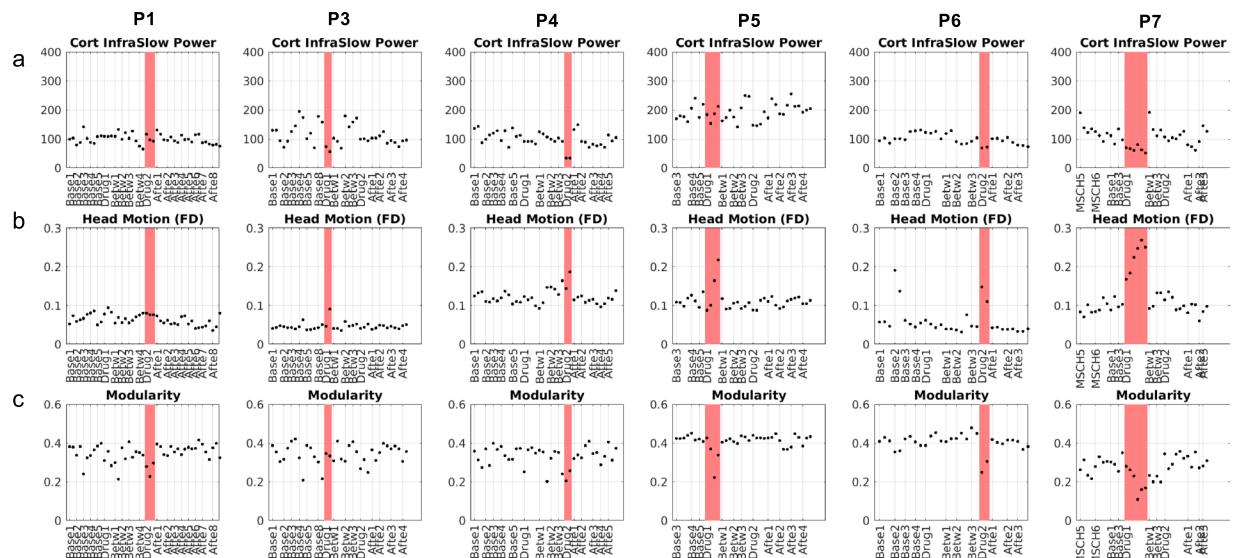


Fig. 6 Quality and signal metrics for PSIL PFM dataset. Each dot represents a resting state scans are shown on the x-axis and red vertical bars depict participants' scans on PSIL. **(a)** Cortical infraslow power (0.009–0.06hz). Drug exposure had no correlation with cortical infraslow power. **(b)** Head motion (also in Fig. 3). **(c)** Newman's modularity. Overall, modularity was lower on PSIL (LME model $P = 1.8754 \times 10^{-9}$) and returned to baseline level after. (LME model $P = 0.68$).

Code availability

Data processing codes for the PSIL PFM data and documentation are uploaded within OpenNeuro. Codes specific to PSIL PFM task analysis and instructions for use can be found at: https://gitlab.com/siegelandthebrain1/PSIL_PFM and OpenNeuro. Software packages incorporated into the above pipelines for data analysis included:

- Matlab R2020b, <https://www.mathworks.com/>
- Cifti matlab utilities (including spin test): <https://github.com/MidnightScanClub/SCAN>
- Connectome Workbench 1.5, <http://www.humanconnectome.org/software/connectome-workbench.html>
- Freesurfer v6.2, <https://surfer.nmr.mgh.harvard.edu/>
- FSL 6.0, <https://fsl.fmrib.ox.ac.uk/fsl/fslwiki>
- 4dfp tools, <https://4dfp.readthedocs.io/en/latest/>

Received: 23 July 2024; Accepted: 13 May 2025;

Published online: 05 June 2025

References

1. Carhart-Harris, R. *et al.* Trial of Psilocybin versus Escitalopram for Depression. *N Engl J Med* **384**(15), 1402–1411 (2021).
2. Davis, A. K. *et al.* Effects of Psilocybin-Assisted Therapy on Major Depressive Disorder: A Randomized Clinical Trial. *JAMA Psychiatry* **78**(5), 481–489 (2021).
3. Goodwin, G. M. *et al.* Single-Dose Psilocybin for a Treatment-Resistant Episode of Major Depression. *N Engl J Med* **387**(18), 1637–1648 (2022).
4. Raison, C. L. *et al.* Single-Dose Psilocybin Treatment for Major Depressive Disorder: A Randomized Clinical Trial. *JAMA* **330**(9), 843–853 (2023).
5. Griffiths, R. R. *et al.* Psilocybin produces substantial and sustained decreases in depression and anxiety in patients with life-threatening cancer: A randomized double-blind trial. *J Psychopharmacol* **30**(12), 1181–1197 (2016).
6. Ross, S. *et al.* Rapid and sustained symptom reduction following psilocybin treatment for anxiety and depression in patients with life-threatening cancer: a randomized controlled trial. *J Psychopharmacol* **30**(12), 1165–1180 (2016).
7. Wilcox, J. A. Psilocybin and Obsessive Compulsive Disorder. *J Psychoactive Drugs* **46**(5), 393–5 (2014).
8. Renelli, M. *et al.* An exploratory study of experiences with conventional eating disorder treatment and ceremonial ayahuasca for the healing of eating disorders. *Eat Weight Disord* **25**(2), 437–444 (2020).
9. Spriggs, M. J. *et al.* Study Protocol for “Psilocybin as a Treatment for Anorexia Nervosa: A Pilot Study”. *Front Psychiatry* **12**, 735523 (2021).
10. Bogenschutz, M. P. *et al.* Clinical Interpretations of Patient Experience in a Trial of Psilocybin-Assisted Psychotherapy for Alcohol Use Disorder. *Front Pharmacol* **9**, 100 (2018).
11. Krebs, T. S. & Johansen, P. O. Lysergic acid diethylamide (LSD) for alcoholism: meta-analysis of randomized controlled trials. *J Psychopharmacol* **26**(7), 994–1002 (2012).
12. Bogenschutz, M. P. *et al.* Percentage of Heavy Drinking Days Following Psilocybin-Assisted Psychotherapy vs Placebo in the Treatment of Adult Patients With Alcohol Use Disorder: A Randomized Clinical Trial. *JAMA Psychiatry* **79**(10), 953–962 (2022).
13. Griffiths, R. R. *et al.* Psilocybin can occasion mystical-type experiences having substantial and sustained personal meaning and spiritual significance. *Psychopharmacology (Berl)*, **187**(3): p. 268–83; discussion 284–92 (2006).
14. Maclean, K. A. *et al.* Factor Analysis of the Mystical Experience Questionnaire: A Study of Experiences Occasioned by the Hallucinogen Psilocybin. *J Sci Study Relig* **51**(4), 721–737 (2012).

15. McCulloch, D. E. *et al.* Psychedelic resting-state neuroimaging: A review and perspective on balancing replication and novel analyses. *Neurosci Biobehav Rev* **138**, 104689 (2022).
16. Wall, M. B. *et al.* Neuroimaging in psychedelic drug development: past, present, and future. *Mol Psychiatry* **28**(9), 3573–3580 (2023).
17. Tagliazucchi, E. *et al.* Increased Global Functional Connectivity Correlates with LSD-Induced Ego Dissolution. *Curr Biol* **26**(8), 1043–50 (2016).
18. Carhart-Harris, R. L. *et al.* Neural correlates of the LSD experience revealed by multimodal neuroimaging. *Proc Natl Acad Sci USA* **113**(17), 4853–8 (2016).
19. Ionescu, T. M. *et al.* Neurovascular Uncoupling: Multimodal Imaging Delineates the Acute Effects of 3,4-Methylenedioxymethamphetamine. *J Nucl Med* **64**(3), 466–471 (2023).
20. Padawer-Curry, J. A. *et al.* Psychedelic 5-HT_{2A} receptor agonism: neuronal signatures and altered neurovascular coupling. *bioRxiv* <https://www.biorxiv.org/content/10.1101/2023.09.23.559145v2.abstract> (2024).
21. Gordon, E. M. *et al.* Precision Functional Mapping of Individual Human Brains. *Neuron* **95**(4), 791–807 e7 (2017).
22. Marek, S. *et al.* Reproducible brain-wide association studies require thousands of individuals. *Nature* **603**(7902), 654–660 (2022).
23. Greene, D. J. *et al.* Integrative and Network-Specific Connectivity of the Basal Ganglia and Thalamus Defined in Individuals. *Neuron* **105**(4), 742–758 e6 (2020).
24. Braga, R. M. & Buckner, R. L. Parallel Interdigitated Distributed Networks within the Individual Estimated by Intrinsic Functional Connectivity. *Neuron* **95**(2), 457–471 e5 (2017).
25. Newbold, D. J. *et al.* Plasticity and Spontaneous Activity Pulses in Disused Human Brain Circuits. *Neuron* **107**(3), 580–589 e6 (2020).
26. Siegel, J. S. *et al.* *Psilocybin desynchronizes brain networks*. medRxiv, (2023).
27. Kargbo, R. B. *et al.* Direct Phosphorylation of Psilocin Enables Optimized cGMP Kilogram-Scale Manufacture of Psilocybin. *ACS Omega* **5**(27), 16959–16966 (2020).
28. Holze, F. *et al.* Pharmacokinetics and Pharmacodynamics of Oral Psilocybin Administration in Healthy Participants. *Clin Pharmacol Ther* **113**(4), 822–831 (2023).
29. Brown, R. T. *et al.* Pharmacokinetics of Escalating Doses of Oral Psilocybin in Healthy Adults. *Clin Pharmacokinet* **56**(12), 1543–1554 (2017).
30. Kimko, H. C., Cross, J. T. & Abernethy, D. R. Pharmacokinetics and clinical effectiveness of methylphenidate. *Clin Pharmacokinet* **37**(6), 457–70 (1999).
31. Donnellan, M. B. *et al.* The mini-IPIP scales: tiny-yet-effective measures of the Big Five factors of personality. *Psychol Assess* **18**(2), 192–203 (2006).
32. Barrett, F. S., Johnson, M. W. & Griffiths, R. R. Validation of the revised Mystical Experience Questionnaire in experimental sessions with psilocybin. *J Psychopharmacol* **29**(11), 1182–90 (2015).
33. Barrett, F. S. *et al.* The Challenging Experience Questionnaire: Characterization of challenging experiences with psilocybin mushrooms. *J Psychopharmacol* **30**(12), 1279–1295 (2016).
34. Roseman, L., Nutt, D. J. & Carhart-Harris, R. L. Quality of Acute Psychedelic Experience Predicts Therapeutic Efficacy of Psilocybin for Treatment-Resistant Depression. *Front Pharmacol* **8**, 974 (2017).
35. Blaimer, M. *et al.* SMASH, SENSE, PILS, GRAPPA: how to choose the optimal method. *Top Magn Reson Imaging* **15**(4), 223–36 (2004).
36. Kundu, P. *et al.* Integrated strategy for improving functional connectivity mapping using multiecho fMRI. *Proc Natl Acad Sci USA* **110**(40), 16187–92 (2013).
37. Moser, J. *et al.* Multi-echo Acquisition and Thermal Denoising Advances Infant Precision Functional Imaging. bioRxiv, (2023).
38. Vizioli, L. *et al.* Lowering the thermal noise barrier in functional brain mapping with magnetic resonance imaging. *Nat Commun* **12**(1), 5181 (2021).
39. Dosenbach, N. U. F. *et al.* Real-time motion analytics during brain MRI improve data quality and reduce costs. *Neuroimage* **161**, 80–93 (2017).
40. Fair, D. A. *et al.* Correction of respiratory artifacts in MRI head motion estimates. *Neuroimage* **208**, 116400 (2020).
41. Flanagan, T. W. & Nichols, C. D. Psychedelics as anti-inflammatory agents. *Int Rev Psychiatry* **30**(4), 363–375 (2018).
42. Bauer, M. E. & Teixeira, A. L. Inflammation in psychiatric disorders: what comes first? *Ann N Y Acad Sci* **1437**(1), 57–67 (2019).
43. Yuan, N. *et al.* Inflammation-related biomarkers in major psychiatric disorders: a cross-disorder assessment of reproducibility and specificity in 43 meta-analyses. *Transl Psychiatry* **9**(1), 233 (2019).
44. Casey, B. J. *et al.* The Adolescent Brain Cognitive Development (ABCD) study: Imaging acquisition across 21 sites. *Dev Cogn Neurosci* **32**, 43–54 (2018).
45. Chiang, C. W. *et al.* Quantifying white matter tract diffusion parameters in the presence of increased extra-fiber cellularity and vasogenic edema. *Neuroimage* **101**, 310–9 (2014).
46. Wang, Y. *et al.* Quantification of increased cellularity during inflammatory demyelination. *Brain* **134**(Pt 12), 3590–601 (2011).
47. Kasper, L. *et al.* The PhysIO Toolbox for Modeling Physiological Noise in fMRI Data. *J Neurosci Methods* **276**, 56–72 (2017).
48. Posner, K. *et al.* Columbia Classification Algorithm of Suicide Assessment (C-CASA): classification of suicidal events in the FDA's pediatric suicidal risk analysis of antidepressants. *Am J Psychiatry* **164**(7), 1035–43 (2007).
49. Moeller, S. *et al.* NOise reduction with DIstribution Corrected (NORDIC) PCA in dMRI with complex-valued parameter-free locally low-rank processing. *Neuroimage* **226**, 117539 (2021).
50. Andersson, J. L., Skare, S. & Ashburner, J. How to correct susceptibility distortions in spin-echo echo-planar images: application to diffusion tensor imaging. *Neuroimage* **20**(2), 870–88 (2003).
51. Zhang, Y., Brady, M. & Smith, S. Segmentation of brain MR images through a hidden Markov random field model and the expectation-maximization algorithm. *IEEE Trans Med Imaging* **20**(1), 45–57 (2001).
52. Andersson, J. L. *Non-linear registration aka spatial normalisation*. FMRIB Centre, (2007).
53. Ciric, R. *et al.* Benchmarking of participant-level confound regression strategies for the control of motion artifact in studies of functional connectivity. *Neuroimage* **154**, 174–187 (2017).
54. Glasser, M. F. *et al.* The minimal preprocessing pipelines for the Human Connectome Project. *Neuroimage* **80**, 105–24 (2013).
55. Power, J. D. *et al.* Methods to detect, characterize, and remove motion artifact in resting state fMRI. *Neuroimage* **84**, 320–41 (2014).
56. Posse, S. *et al.* Enhancement of BOLD-contrast sensitivity by single-shot multi-echo functional MR imaging. *Magn Reson Med* **42**(1), 87–97 (1999).
57. Fischl, B. *et al.* High-resolution intersubject averaging and a coordinate system for the cortical surface. *Hum Brain Mapp* **8**(4), 272–84 (1999).
58. Gratton, C. *et al.* Functional Brain Networks Are Dominated by Stable Group and Individual Factors, Not Cognitive or Daily Variation. *Neuron* **98**(2), 439–452 e5 (2018).
59. Raut, R. V. *et al.* On time delay estimation and sampling error in resting-state fMRI. *Neuroimage* **194**, 211–227 (2019).
60. Newman, M. E. Modularity and community structure in networks. *Proc Natl Acad Sci USA* **103**(23), 8577–82 (2006).
61. Rubinov, M. & Sporns, O. Complex network measures of brain connectivity: uses and interpretations. *Neuroimage* **52**(3), 1059–69 (2010).
62. *Psilocybin Precision Functional Mapping (data from Psilocybin desynchronizes the human brain)* <https://openneuro.org/datasets/ds006072/> (2025).

63. Gorgolewski, K. J. *et al.* The brain imaging data structure, a format for organizing and describing outputs of neuroimaging experiments. *Sci Data* **3**, 160044 (2016).
64. Carhart-Harris, R. L. *et al.* Neural correlates of the psychedelic state as determined by fMRI studies with psilocybin. *Proc Natl Acad Sci USA* **109**(6), 2138–43 (2012).
65. Daws, R. E. *et al.* Increased global integration in the brain after psilocybin therapy for depression. *Nat Med* **28**(4), 844–851 (2022).

Acknowledgements

We are grateful to our study participants, who completed a demanding protocol for the benefit of scientific investigation. This work was supported by the Taylor Family Institute Fund for Innovative Psychiatric Research (J.S.S., T.O.L., G.E.N.), McDonnell Center for Systems Neuroscience (J.S.S., G.E.N.), Institute of Clinical and Translational Science (G.E.N.), National Institutes of Health grants MH112473 (J.S.S., S.S., C.H., G.E.N.), T32 DA007261 (J.S.S.), MH129616 (T.O.L.), MH121276 (N.U.F.D.), MH096773 (N.U.F.D.), MH122066 (N.U.F.D.), MH124567 (N.U.F.D.), NS129521 (N.U.F.D.), and NS088590 (N.U.F.D.); the Intellectual and Developmental Disabilities Research Center (N.U.F.D.); by the Kiwanis Foundation (N.U.F.D.); the Washington University Hope Center for Neurological Disorders (NUFD); and by Mallinckrodt Institute of Radiology pilot funding (NUFD). Additionally, this study utilized data from the ABCD study, supported by NIH grant U01DA041120.

Author contributions

Conception: J.S.S. and G.E.N. Study design: J.S.S., S.S., T.O.L., E.J.L., A.Z.S. and G.E.N. Data acquisition and processing: J.S.S., S.S., T.R.R., D.P., R.C., C.H. and A.Z.S. Data analysis and interpretation: J.S.S., S.S., T.O.L., R.C., N.M., N.U.F.D., G.E.N. and N.U.F.D. Manuscript writing and revision: S.S., J.S.S., R.C., G.E.N. Participant 7 was author N.U.F.D.

Competing interests

Within the last two years, author JSS was an employee of Sumitomo Pharma America and received consulting fees from Longitude Capital. Author GEN has served as principal or co-investigator on studies funded by Alkermes, Inc., LB Pharmaceuticals and COMPASS Pathways, and has received research support from Usona Institute (drug only). She has served as a paid consultant for Carelon and Alkermes, Inc. AZS is a consultant for Soraneuroscience, LLC. NUFD is a co-founder of Turing Medical Inc, and may benefit financially if the company is successful in marketing FIRMM motion monitoring software products and may receive royalty income based on FIRMM technology developed at Washington University School of Medicine (WUSOM) and licensed to Turing Medical Inc.

Additional information

Supplementary information The online version contains supplementary material available at <https://doi.org/10.1038/s41597-025-05189-0>.

Correspondence and requests for materials should be addressed to S.S. or J.S.S.

Reprints and permissions information is available at www.nature.com/reprints.

Publisher's note Springer Nature remains neutral with regard to jurisdictional claims in published maps and institutional affiliations.



Open Access This article is licensed under a Creative Commons Attribution-NonCommercial-NoDerivatives 4.0 International License, which permits any non-commercial use, sharing, distribution and reproduction in any medium or format, as long as you give appropriate credit to the original author(s) and the source, provide a link to the Creative Commons licence, and indicate if you modified the licensed material. You do not have permission under this licence to share adapted material derived from this article or parts of it. The images or other third party material in this article are included in the article's Creative Commons licence, unless indicated otherwise in a credit line to the material. If material is not included in the article's Creative Commons licence and your intended use is not permitted by statutory regulation or exceeds the permitted use, you will need to obtain permission directly from the copyright holder. To view a copy of this licence, visit <http://creativecommons.org/licenses/by-nc-nd/4.0/>.

© The Author(s) 2025